Study of a sealed high gas pressure THGEM detector and response of alpha particle spectra*

Yu-Ning Zhang(张宇宁)[1] Qian Liu(刘倩)[1,2;1)] Hong-Bang Liu(刘宏邦)[3;2)] Yi-Gang Xie(谢一冈)[1,4]
Xiao-Rui Lyu(吕晓睿)[1,2] Shi Chen(陈石)[1] Wen-Qian Huang(黄文谦)[1] Dao-Jin Hong(洪道金)[1]
Yang-Heng Zheng(郑阳恒)[1,2]

[1] University of Chinese Academy of Sciences, Beijing 100049, China
[2] CAS Key Laboratory of Vacuum Physics, UCAS, Beijing 100049, China
[3] Guangxi Key Laboratory for the Relativistic Astrophysics, Guangxi University, Nanning 530004, China
[4] Institute of High Energy Physics, Chinese Academy of Sciences, Beijing 100049, China

Abstract: A sealed high gas pressure detector working in pure argon is assembled. It consists of a 5 cm × 5 cm PCB THGEM (THick Gaseous Electron Multiplier). The detector structure and experimental setup are described. The performance under high pressure (2 atm) is examined, selecting optimal voltages for the ionization region and induction region. The dependence of the shape of alpha particle spectra measured with relative gas gain on gas pressure (1.3–2.0 atm) has been studied. Eight data sets of relative gas gain versus working voltage of THGEM, expressed by weighting field E/P, are normalized, consistent with theory. The results show that the air tightness of the chamber is good, measured by a sensitive barometer and checked with gas gain. The experimental results are compared with Monte Carlo simulation of energy deposition without gas gain involved.

Keywords: THGEM, sealed detector, long-term gain stability, alpha particle

PACS: 29.40.Cs, 29.40.-n **DOI:** 10.1088/1674-1137/41/4/046001

1 Introduction

Gaseous detectors have been widely used in collider physics and other science frontier experiments due to their large volume, good spatial resolution and reasonable cost. Classically, most gaseous detectors need to be flushed by continuous working gas. In some special fields, for instance, astrophysics or outdoor applications, the cumulative volume is limited while good performance of the detector is required. A sealed gaseous detector is one candidate to meet those requirements.

The THick Gaseous Electron Multiplier (THGEM) [1–3], an "expanded" GEM explored by A. Breskin et al in 2004, can be produced economically, mainly using printed circuit board (PCB). In recent years, some new substrates (ceramic and liquid crystal polymer (LCP) etc) and new technologies (laser hole-drilling and chemical etching) have developed very rapidly. THGEMs are robust, low cost and easy to manufacture, with high gain (10^3–10^5), good spatial resolution (sub-mm), high counting rate, and good stability. A special type of thinner-THGEM [4–6] was developed domestically in 2011.

For a sealed gaseous detector, one of the most important issues is to keep the parameters of the working gas as constant as possible. Therefore, our first task is to study the long-time stability of the inner working gas of the sealed chamber. In general, the air tightness of the sealed detector and the outgassing rate of the detector materials influence the long-time stability.

To test the air tightness of the detector, a barometer is used to monitor changes in the detector gas pressure. An alpha source, ^{241}Am, placed inside the detector, is used both for checking gas pressure by measuring the gas gain information from the alpha spectra, and for further studying the dependence of alpha spectra on gas pressure.

Spectrum sizes are important for different particles, including heavy particles, light particles and photons of different energies. For the next step in developing novel detectors, in particular for non-ageing gaseous detectors for visible light, using pure argon is crucial [7, 8]. In addition, to have the detector working under high gas pressure is very advantageous to improve the detection

Received 22 September 2016, Revised 23 November 2016
* Supported by National Natural Science Foundation of China (11575193, 11205240, 11265003, U1431109)
1) E-mail: liuqian@ucas.ac.cn
2) E-mail: liuhb@gxu.edu.cn

efficiency and spatial resolution and to catch more effective track lengths in the fiducial volume of the detector [9, 10].

The response of the deposited energy distribution of alpha particles with their spectrum, influenced by source-chamber geometry and gas pressure, should be known for any heavy particles and light particles required in related experiments. Some authors have focused on alpha particles in environmental ambient gas [11], on the geometrical relationship between source and collective electrodes of the chamber [12], on UV photons under low temperature [13], on alpha spectra in different rare gases [14], on the deposited energy distribution within different Bragg's curve sections for alphas and on adjusting the optimal ionization thickness for heavy particles [15]. All these issues show the significance of this field of detector studies.

This paper focuses on the parameters of a THGEM detector working in high pressure pure Ar, the related techniques for keeping air tightness, the shapes of alpha spectra under different high pressures, the long term stability, and the gas gain influenced by gas pressure. Monte Carlo simulations with GEANT4 software [16] and calculations are compared with the experimental results.

2 Experimental setup

As illustrated in Fig. 1, a sealed gaseous detector based on THGEM has been built. The key device of the detector is a single layer of 5 cm × 5 cm PCB THGEM board, 200 μm thick, clad with 18 μm of copper and plated with gold layers on the top of the Cu film. The holes are cylindrical (diameter 200 μm) with 500 μm pitch. They were produced at the University of Chinese Academy of Sciences (UCAS) and the Second Academy of China Aerospace Science and Industry Corporation (CASIC). The structure and characteristics of the THGEM can be found in Ref. [6]. The distance between the cathode mesh and the upper layer of the THGEM, which is the drift region, is 1.5 cm, while the distance between the lower layer of the THGEM and the anodes, which is the induction region, is 0.3 cm.

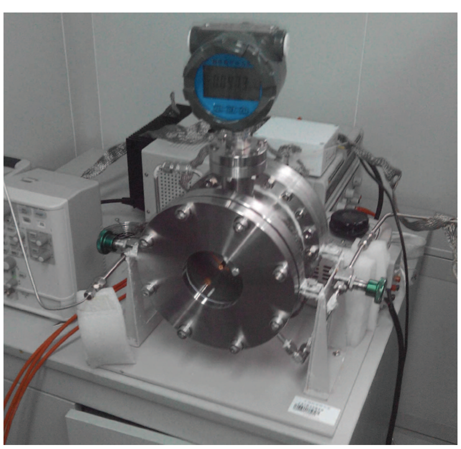

Fig. 1. (color online) The sealed detector.

The shell of the detector is a stainless-steel cylindrical vessel. The chamber is sealed by vacuum flanges tightly connected with oxygen-free copper and rubber rings. There are 8 Kovar electrodes on the bottom flange, which are used for providing high voltage feedthrough. The anode's readout consists of a vacuum multi-pin plug-and-socket designed to meet future purposes, and temporarily being connected as one output. The front end window is comprised of an ordinary glass of dimensions ∅8×0.8 cm. The glass is tightly pressed to the stainless-steel chamber by Teflon. With the glass window, the detector is able to detect outer sources, especially designed for visible light. Two precise aciculiform valves are used on both sides of the flanges to guarantee the air tightness. The chamber leakage was checked with a He gas probe and de-aerated at 100 ℃ after being assembled. The result shows that the vacuum degree of the chamber can reach 10^{-5} Pa, and the leak rate of the chamber is less than 10^{-10} Pa×m^3/s. The various parts of the sealed detector are easy to assemble, as shown in Fig. 2.

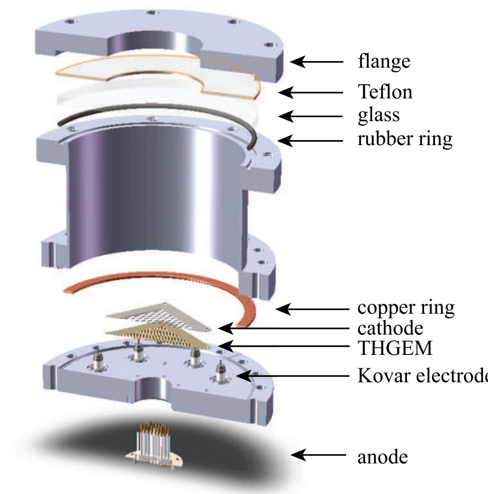

Fig. 2. (color online) The structure of the sealed chamber.

The high voltages on the electrodes are provided by a CAEN NDT1471H HV programmable power supply which provides 4 independent High Voltage channels. The signals are recorded by a CR110 pre-amplifier (charge sensitivity 1.4 V/pC) followed by a CAEN N968 spectroscopy amplilier (shaping time is 0.5 μs, amplification factor is 100) and a CAEN N957 8K Multi-Channel Analyzer (MCA, range $0-10$ V). A schematic diagram of the structure of the detector test setup is shown in Fig. 3.

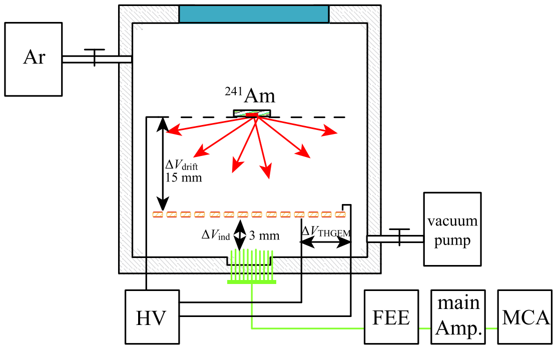

Fig. 3. (color online) Schematic diagram of the experimental setup.

To test the long-time stability of the detector, an alpha source ^{241}Am of 0.8 μCi was fixed at the centre of the cathode with an iron wire, as shown in Fig. 3. For ^{241}Am, the half-life is about 433 years, so the activity is almost constant during the experiment. Those particles are emitted into the drift region with a solid angle of 2π. During the whole period of the experiment, the spectra of alpha particles was measured each day. The relative value of the chamber gas pressure compared to the ambient atmosphere was measured by a barometer connected to the chamber via a CF35 flange. The resolution of the barometer is 2.5 kPa. The gain of the detector could alsob e affected by environmental factors such as temperature and humidity [17–19], so these were monitored by a sensor.

3 Experimental results and discussion

3.1 Performance study under high pressure

In order to guarantee safety, especially to avoid the glass window being broken, testing the strength of the detector chamber under pressure is the first step. The chamber was evacuated to 10^{-9} atm (1 atm $= 1.014\times10^5$ Pa) by molecular pump, and filled with pure Ar to 2.0 atm. Voltages were then applied successively to all the electrodes.

The performance tests under high pressure mainly consist in selecting optimal voltages in the ionization region $\Delta V_{\rm drift}$ and induction region $\Delta V_{\rm ind}$.

At the beginning, a typical MCA spectra of alpha particles was measured at 2.0 atm, shown in Fig. 4 with $\Delta V_{\rm drift} = 400$ V, $\Delta V_{\rm THGEM} = 700$ V and $\Delta V_{\rm ind} = 600$ V. Except for the low range electronics noise, a pulse peak is clearly seen. The gas gain of the detector can be represented by the channel number of the position of the pulse peak.

From the relative gain (channel number) versus the drift voltage ($\Delta V_{\rm drift}$) under the same working voltage ($\Delta V_{\rm THGEM} = 700$ V) and the same induction voltage ($\Delta V_{\rm ind} = 600$ V), shown in Fig. 5, the optimum $\Delta V_{\rm drift}$ is 400 V with respect to the maximum gas gain. For Fig. 5, the curve is caused by two factors. With increasing $\Delta V_{\rm drift}$, the recombination effect reduces, and more primary ionized electrons appear. The other factor is that with increasing $\Delta V_{\rm drift}$, the efficiency of electrons entering holes on the upper layer of the THGEM reduces.

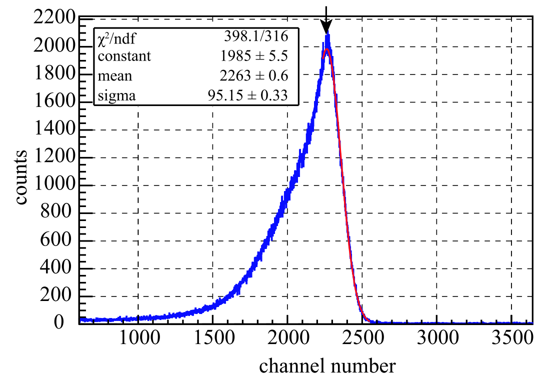

Fig. 4. (color online) A typical MCA spectrum measured by the detector at 2.0 atm.

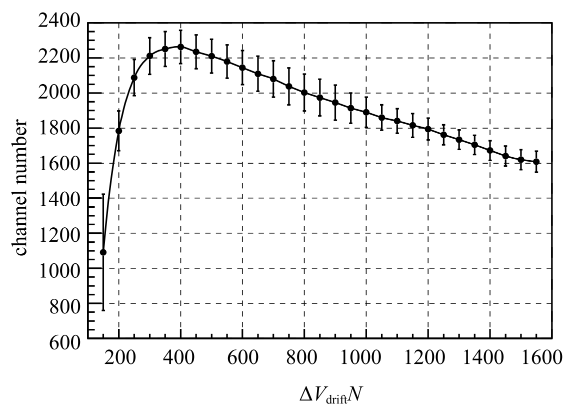

Fig. 5. (color online) The channel number of the pulse peak positions changes with $\Delta V_{\rm drift}$ under fixed $\Delta V_{\rm THGEM}$ and $\Delta V_{\rm ind}$.

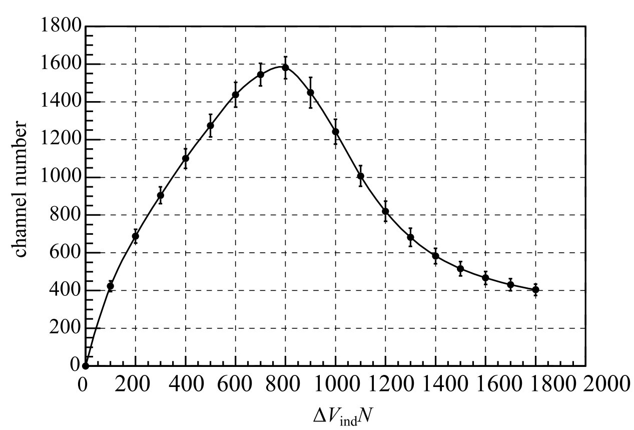

Fig. 6. The channel number of the pulse peak changes with $\Delta V_{\rm ind}$ under fixed $\Delta V_{\rm THGEM}$ and $\Delta V_{\rm drift}$.

As illustrated in Fig. 6, the relative gains of the different $\Delta V_{\rm ind}$ under $\Delta V_{\rm THGEM}=600$ V and $\Delta V_{\rm drift}=400$ V are measured. Due to the special structure of the anode, an optimal value of $\Delta V_{\rm ind}$ exists. The gas gain of the THGEM is also positively correlated with electron collection efficiency [21–23]. Due to the effect of ion back flow, the electron collection efficiency will not always improve with increasing $\Delta V_{\rm ind}$.

3.2 Alpha particle spectra under various gas pressure

The ^{241}Am source emits alpha particles with energies of $\sim$ 5.486 MeV ($\sim$ 85.2%) and $\sim$ 5.443 MeV ($\sim$ 12.8%) [24]. For the 5.486 MeV alpha particles, their range in ordinary air is $\sim$ 3.5 cm. According to the Bragg-Kleeman rule, the estimated range of the alpha particles in normal temperature-pressure Ar is $\sim$ 4.26 cm. For the ^{241}Am source located at the top centre of the cathode surface, only some of the deposited energy of the alpha particles is caught in the fiducial volume. This means that if alpha particles are required to completely ionize in the drift region, the pressure of the detector should be increased. To verify this deduction, the MCA spectra of alpha particles for different values of gas pressure were obtained.

A series of alpha-ray spectra of 8 groups of various pressures (1.3–2.0 atm) under 5 different $\Delta V_{\rm THGEM}$ were measured during 6 hours of stable environment conditions (see Appendix A).

Two MCA spectra of alpha particles measured at 1.3 atm and 2.0 atm are shown in Fig. 7 and Fig. 8 respectively, in which the three groups of voltages are the same ($\Delta V_{\rm drift}=400$ V, $\Delta V_{\rm THGEM}=600$ V and $\Delta V_{\rm ind}=600$ V). In Fig. 9, there is an obvious trend where, under the same $\Delta V_{\rm THGEM}$, the higher the pressure of the chamber ($1.8-2.0$ atm), the smaller the gas gain.

Figure 7 and Fig. 8 are explained as follows:

1) With decreasing pressure, some of the alpha particles escape out of the fiducial (sensitive) volume from the lateral sides, and double peaks appear, just caused by the shorter remainimg tracks (Fig.7).

2) When the pressure is very high, all particles stop (including Bragg's tail) in the fiducial volume, and a single peak appears (Fig. 8).

2) From 8 data sets at various pressures (1.3–2.0 atm), the evolutional tendency of the alpha spectra sizes is obvious: both peak (max channel) and starting point (min channel) with a valley between two peaks decrease, i.e. shift to lower channels with increasing pressure. Figure 9 summarizes the channel number changes with $\Delta V_{\rm THGEM}$ under 3 different pressures. These results could be explained by 2 factors: firstly, even more energy is deposited in the fiducial volume with increasing pressure (dE/dx proportional to gas density); secondly, the gas gain is a function of weighting electric field strength E/p, being smaller in the THGEM holes. This effect causes a decrease of gas gain, which would be the dominant factor compared to the first.

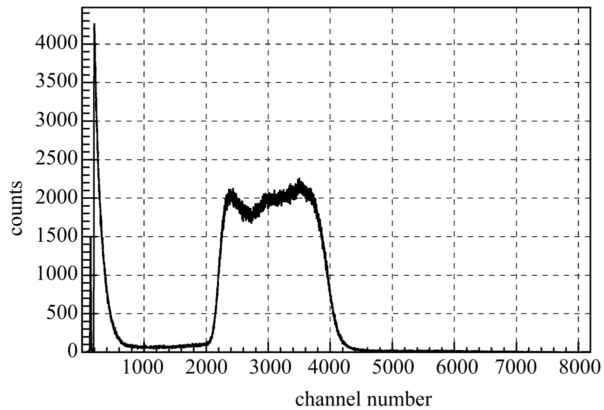

Fig. 7. The MCA spectrum of alpha particles measured at 1.3 atm.

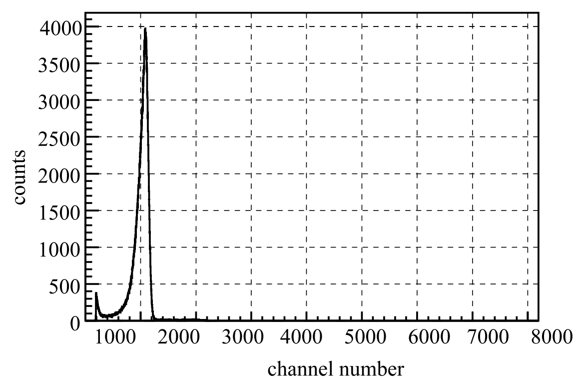

Fig. 8. The MCA spectrum of alpha particles measured at 2.0 atm.

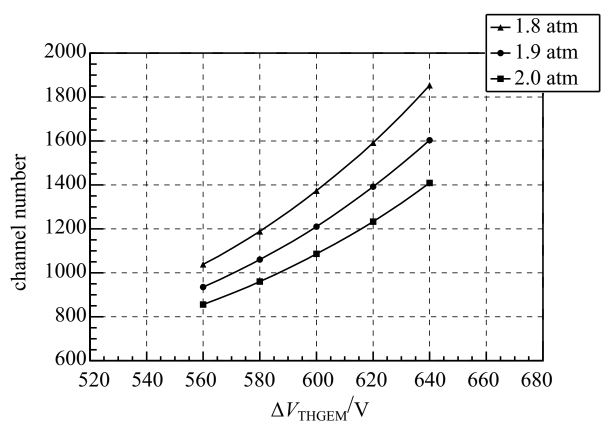

Fig. 9. At different inner pressure of the chamber, the channel number of the pulse peak changes with $\Delta V_{\rm THGEM}$.

From the gas amplification theory developed by Townsend [25], the gas amplification coefficient, or gas gain M in high electric field is related to the first Townsend ionization coefficient α_T. $1/\alpha_T$ is the mean free path between ionizing collisions. In a rough approximation, the avalanche multiplication of electrons in THGEM can be deduced by using the parallel-plate approach as $\ln M/(Pd)$, where d is the interelectrode distance and P is the pressure, i. e. the weighting electric field of the THGEM is $E/P \approx \Delta V_{\text{THGEM}}/(Pd)$, as done in Ref. [8]. For 40 spectra with 8 sets at different pressures, the gas gain can be represented by the channel number N_{Ch} of the pulse peak (for spectra with two peaks, the right one is selected). Values of $\ln N_{\text{Ch}}/(Pd)$ as a function of the weighting electric field $V_{\text{THGEM}}/(Pd)$ are shown in Fig. 10. The tendency of $\ln N_{\text{Ch}}/(Pd)$ corresponding to gas amplification changing with the weighting electric field is expressed as normalized linearity.

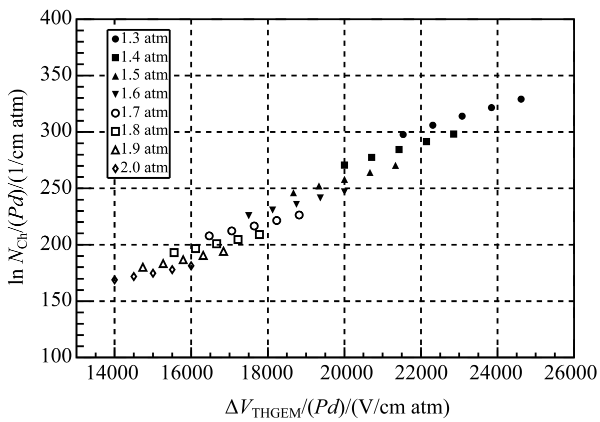

Fig. 10. Formulae for $\Delta V_{\text{THGEM}}/(Pd)$ and for the relative gas amplification expressed in the form $\ln N_{\text{Ch}}/(Pd)$.

3.3 Long term stability and gas gain response

To study the long-time stability of gain, we repeatedly obtained the spectra of alpha particles measured by the detector working at 1.5 atm during a long term period. Under the conditions of $\Delta V_{\text{THGEM}} = 600$ V, $\Delta V_{\text{drift}} = 1000$ V and $\Delta V_{\text{ind}} = 600$ V, the MCA spectrum of alpha particles had a pulse peak like Fig. 4. Considering that the temperature or other environmental factors might affect the gas gain, the experiment was run during a period of days with stable environmental conditions. Under these conditions, the gain rose by $\sim 5\%$ during 7 days, as shown in Fig. 11.

With the barometer (specification 2.5 kPa) and the temperature sensor (specification 0.5 ℃), the definite gas density of the sealed chamber was obtained during this period. The change of p/T within 18 days was within the measurement error of 8.4 kPa/K. This means that the leakage of the chamber is very low.

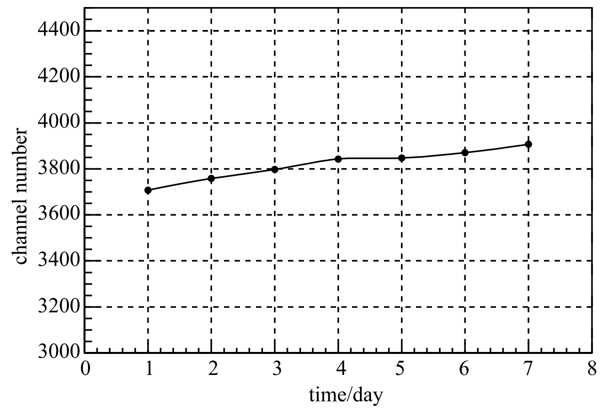

Fig. 11. The channel number of the pulse peak measured by the detector at 1.5 atm changes with time, under the conditions of $\Delta V_{\text{THGEM}} = 600$ V, $\Delta V_{\text{drift}} = 1000$ V ang $\Delta V_{\text{ind}} = 600$ V.

In Fig. 9, the pressure changes from 2.0 atm to 1.9 atm, and the gas gain rises $\sim 11.4\%$. Roughly, if the pressure changes by 0.01 atm, the gain changes by 1%. Concerning the gas gain changing over a relatively long time (7 days), the gas gain slightly increases with time, as shown in Figure. 11. This tendency could be explained by several factors. One factor is a small leakage influencing the weighting field in the chamber. Therefore, if the change of the gas gain could be controlled within $\sim 10\%$, the stable period of the detector would be about 14 days. In addition, further long-term stability should be considered with the discharge and the outgas of the inner material of the chamber.

4 Monte Carlo simulation and calculations

To compare the different tendencies between experimental alpha spectra size obtained by gas gain, energy deposition spectra were obtained by GEANT4 simulation with 5.486 MeV alpha particles deposited in the fiducial volume of pure Ar at 3 different pressures, as shown in Fig. 12. The emitted particles were set to come from a point source at the centre of the upper surface of the fiducial volume with a solid angle of 2π.

As Fig. 12 shows, almost all the energy of the alpha particles is deposited in the pure Ar at 2.0 atm. However, for lower gas pressure, for instance, 1.0 atm or 1.5 atm, considerable numbers of alpha particles do not lose all of their energy. For 1.0 atm, there is not even a peak at 5.486 MeV, but two peaks at lower energies. Obviously, for most alpha particles, the energy deposited associated with the tracks in the fiducial volume could only cover parts of their ranges. As the pressure increases, more and more tracks involve the whole ranges of the alpha particles. This will form the peak at 5.486 MeV in the energy spectrum. Accordingly, the counts of the tracks in the lower energy region with two peaks gradually reduce and the peaks shift to the high energy region, with a small part remaining, shown as the green histogram of 2.0 atm in Fig. 12. All these results are consistent with those obtained from experiments, but without the influence of gas gain.

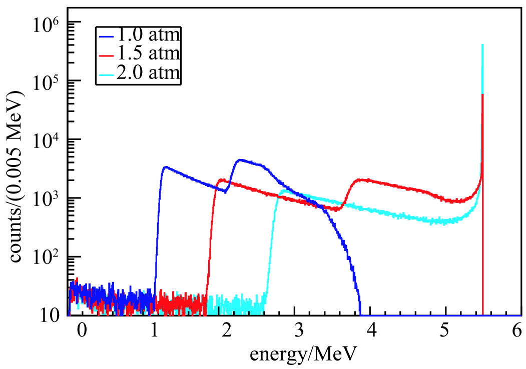

Fig. 12. (color online) The simulated energy spectra of the alpha particles deposited in the fiducial volume at 3 different pressures.

In the case of considering the tracks of alpha particles which only point to the circular disc, and ignoring those pointing to the lateral side or the corner of the drift region, the energy spectrum estimated by GEANT4 simulation is the red histogram shown in Fig. 13. The start of the energy spectrum, shown as the peak, is due to the effect of the shortest tracks, and the end part is contributed by the longest tracks, which end at the edge of the circular disc. The contribution of the tracks which point to the lateral side and the corner of the drift region are shown by the green histogram in Fig. 13. An extra bump distribution appears at the largest MCA channel region, contributed by thee longest tracks which end at the corners of the rectangular fiducial volume. By combining these two histograms to form the blue histogram in Fig. 13, all the tracks are included in the fiducial volume. The blue histogram has been obtained independently with all tracks in the whole fiducial volume.

Different from the complicated rectangular fiducial volume, only a simple circular disc is considered, and the solid angle Ω of a point source from the top center to the circular disc could be given by the following formula:

$$\Omega = 2\pi\left(1-\frac{h}{\sqrt{R^2+h^2}}\right), \tag{1}$$

where R is the radius of the circular disc, and h is the height from the point source to the circular disc. The length from the point source to the edge of the circular disc is $l=\sqrt{R^2+h^2}$, thus the differential is

$$\frac{\mathrm{d}\Omega}{\mathrm{d}l} = \frac{\mathrm{d}\Omega}{\mathrm{d}R}\frac{\mathrm{d}R}{\mathrm{d}l} = 2\pi\cdot\frac{Rh}{(R^2+h^2)^{3/2}}\frac{l}{\sqrt{l^2-h^2}} = 2\pi\cdot\frac{h}{l^2} \tag{2}$$

where $R \leqslant 2.5$ cm and $h = 1.5$ cm. The differential changes with l, as Fig. 14 shows. From Fig. 14, a large peak appears at the start point, then the curve gradually decreases with increasing l, before finally cutting off at the circular edge.

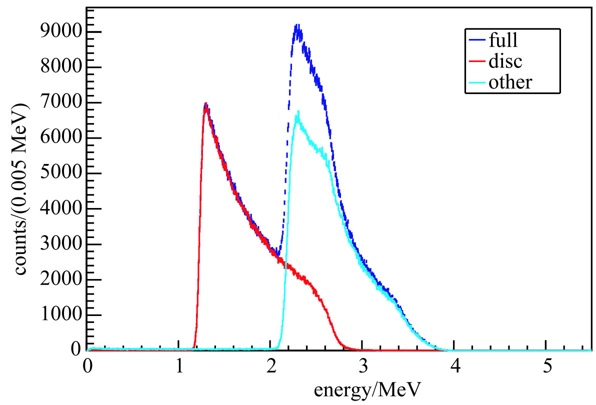

Fig. 13. (color online) Energy distribution of all tracks in the fiducial volume at 1.0 atm pressure, estimated by GEANT4 simulation.

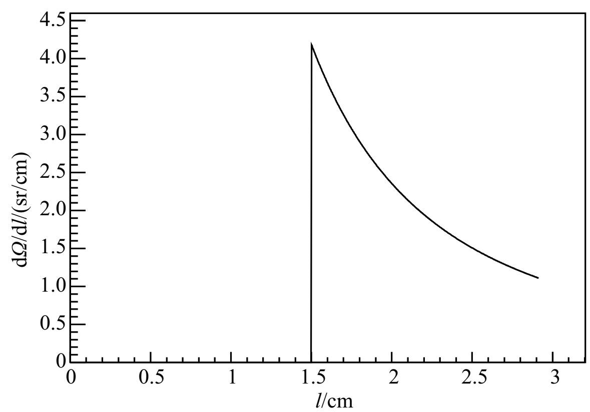

Fig. 14. $R \leqslant 2.5$ cm and $h = 1.5$ cm. The differential changes with l.

$\mathrm{d}N/\mathrm{d}l = (\mathrm{d}N/\mathrm{d}\Omega)\cdot(\mathrm{d}\Omega/\mathrm{d}l)$, where N is the number of the source, and $\mathrm{d}N/\mathrm{d}\Omega$ is a homogeneous distribution ($\mathrm{d}N/\mathrm{d}\Omega = N_0/2\pi$, where N_0 is the initial value of N). Finally, this $\mathrm{d}N/\mathrm{d}l$ just represents the alpha spectra, with constant $\mathrm{d}E/\mathrm{d}x$ along l. It coincides with Fig. 13. After some factors including Bragg curve and non-point source size with film coating have been revised, this $\mathrm{d}N/\mathrm{d}l$ should be more precisely consistent with the experimental results.

5 Conclusion and prospects

In summary, the performance under high pressure of 2 atm and the stability of the sealed chamber with an ^{241}Am source have been studied, and the relationship between the shape of alpha particle spectra measured with gas gain and gas pressure has been studied and analyzed in detail. Eight sets of data points for relative gas gain versus working voltage of THGEM under 1.3–2.0 atm, expressed by weighting field E/P, were normalized, being consistent with theory.

The stability of long-term gas pressure has been monitored. The pressure changes from 2.0 atm to 1.9 atm with the gas gain rising $\sim$ 11.4%. This tendency has been compared with Monte Carlo simulation of energy deposition without gas gain involved. This is helpful for further study and application of the performance of sealed chambers.

For the next step, to answer whether the gain fall with time is caused by outgassing or some other factors, some special instruments such as a Residual Gas Analyzer (RGA) will be used to analyze the change of the components of the working gas. In addition, to restrain outgassing of the chamber, some actions could be taken, such as baking the chamber under vacuum conditions and changing the THGEM substrate to one with a lower outgassing effect.

Both sealed and high gas pressure THGEM detectors could have broad scale applications with different kinds of particles. Based on the results of this experiment, the use of THGEMS in gas avalanche photomultipliers to detect UV or visible light, time projection chambers used in collider physics, and other applications in the field which need high pressure and sealed chambers, should be explored in the future.

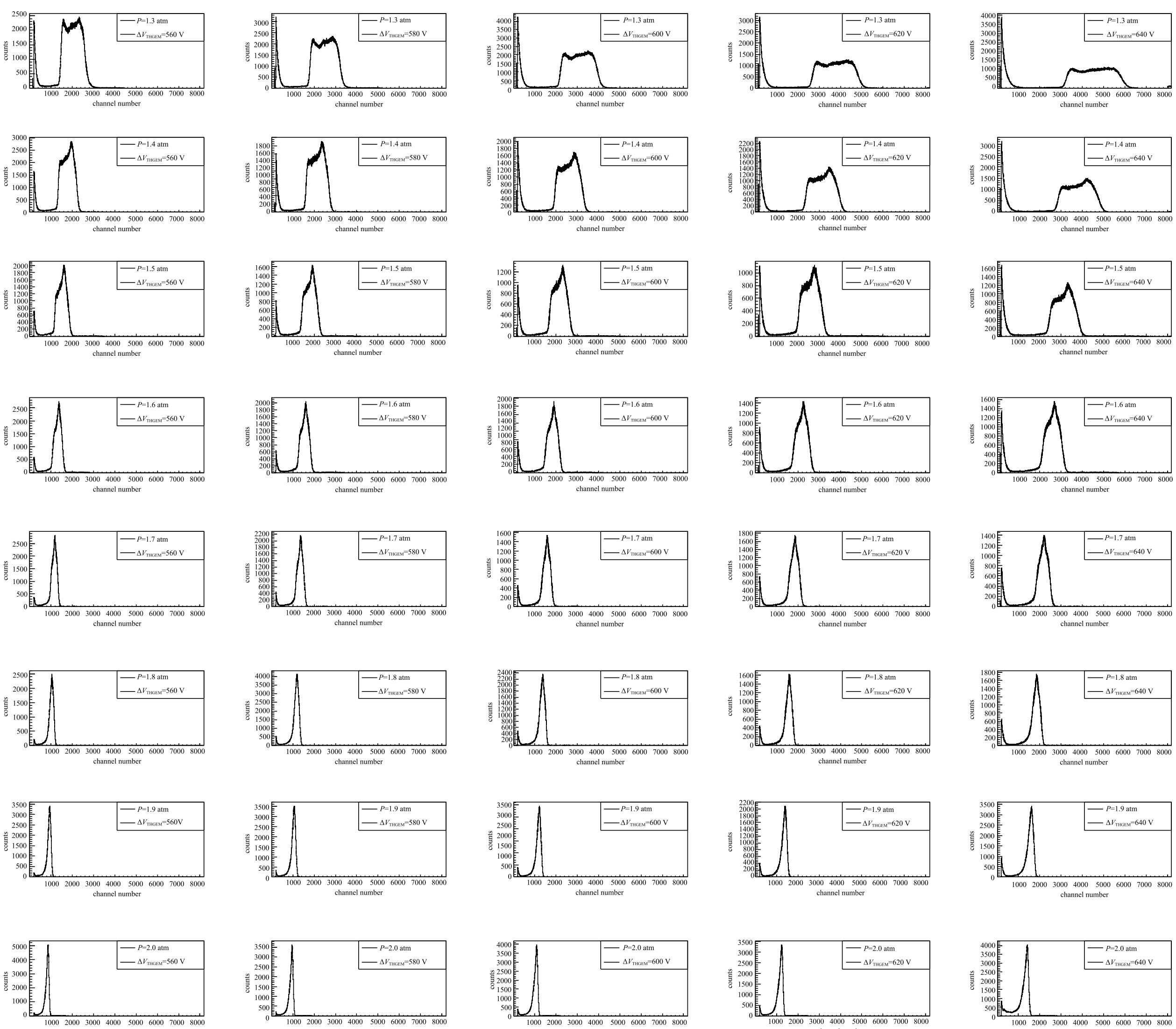

Fig. 15. The MCA spectra of alpha particles for different values of gas pressure.

References

1 R. Chechik et al, Nucl. Instrum. Methods A, **535**: 303–308 (2004)
2 C. Shalem et al, Nucl. Instrum. Methods A, **558**: 475–489 (2006)
3 A. Breskin et al, Nucl. Instrum. Methods A, **598**: 107–111 (2009)
4 H. B. Liu et al, Nucl. Instrum. Methods A, **659**: 237–241 (2011)
5 H. B. Liu et al, JINST, **7**: C06001 (2012)
6 Q. Liu et al, JINST, **8**: C11008 (2013)
7 A. Bressan et al, Nucl. Instrum. Meth. A, **423**: 119–124 (1999)
8 A. Buzulutskov et al, Nucl. Instrum. Meth. A, **433**: 471–475 (1999)
9 A. S. Korff, *Electron and Nuclear Counters* (New York: Van-Nostrand, 1955)
10 F. Sauli, *Principles of operation of multiwire proportional and drift chambers*, CERN-77-09 (1977)
11 G. Charpak et al, JINST, **3**: P02006 (2008)
12 H. B. Xue et al, Proceedings of the 4th National Conference on Nuclear Monitoring (1999) (in Chinese)
13 B. L. Paredes et al, JINST, **10**: P07017 (2015)
14 K. Saito et al, IEEE Transactions on Nuclear Science, **49**(4): 1674–1680 (2002)
15 D. Y. Kim et al, Journal of the Korean Physical Society, **68**: 1060–1068 (2016)
16 S. Agostinelli et al, Nucl. Instrum. Methods A, **506**: 250–303 (2003)
17 F. D. Amaro et al, Nucl. Instrum. Methods A, **579**: 62–66 (2007)
18 J. Dong et al, Chinese Phys. B, **18**: 4299–4233 (2009)
19 X. K. Zhou et al, Chin. Phys. Lett, **31**(3): 032901 (2014)
20 H. B. Liu et al, Chin. Phys. C, **35**(4): 363–367 (2011)
21 F. Sauli et al, Nucl. Instrum. Methods A, **560**: 269–277 (2006)
22 M. Alexeev et al, JINST, **8**: P01021 (2013)
23 B. L. Wang et al, Chin. Phys. Lett, **31**(12): 122901 (2014)
24 Data for the ^{241}Am source. https://en.wikipedia.org/wiki/Americium#cite_note-92
25 B. Sitar et al, *Ionization Measurements in High Energy Physics* (Berlin: Springer, 1993), p. 89